

# Two components for one resistivity in $\text{LaVO}_3/\text{SrTiO}_3$ heterostructure

H. Rotella,<sup>1</sup> O. Copie,<sup>1</sup> A. Pautrat,<sup>1</sup> P. Boullay,<sup>1</sup> A. David,<sup>1</sup> D. Pelloquin,<sup>1</sup> and W. Prellier<sup>1</sup>

<sup>1</sup>*Laboratoire CRISMAT, CNRS UMR 6508, ENSICAEN et Université de Caen,  
6 Bd Maréchal Juin, 14050 Caen Cedex 4, France.*

(Dated: April 1, 2014)

A serie of  $\text{LaVO}_3$  thin films have been prepared on (001)-oriented  $\text{SrTiO}_3$  substrates using the Pulsed Laser Deposition (PLD) technique. Transport properties are dominated by large sheet carrier density and large electronic mobility and non linear Hall effect is characteristic of a two carriers material. In addition, a cross-over from a semiconducting state at high-temperature to a metallic state at low-temperature is observed, with a clear enhancement of the metallic character as the growth temperature. We show that activated diffusion of oxygen vacancies in the  $\text{SrTiO}_3$  substrate is the major process which causes the metallicity, and the film-substrate assembly behaves accordingly as an original semiconducting-metallic parallel resistor.

PACS numbers: 81.15.Fg, 68.55.A-, 61.05.cp

The discovery of a conducting and superconducting behaviors when stacking together the two band insulators  $\text{LaAlO}_3$  (LAO) and  $\text{SrTiO}_3$  (STO) has motivated intense research activities to understand these phenomena<sup>1-3</sup>. The genuine origin of the highly mobile charge carriers has been a central point of the debate, with models focusing on electronic reconstruction at the interface due to a polar discontinuity between the two insulators<sup>2-5</sup>, on cation intermixing or on oxygen vacancies<sup>6-8</sup>. It has been shown that 2D electronic conduction behavior can be observed for peculiar controlled conditions. In particular, oxygen pressure used for the film growth and annealing conditions are crucial parameters to tune the amount of oxygen vacancies and the dimensionality of transport properties<sup>9,10</sup>. Using a Mott insulator with strong coulomb interactions instead of a band insulator should allow to take advantage of rich properties of electronic correlated systems<sup>11</sup>, and other systems such as  $\text{LaTiO}_3/\text{SrTiO}_3$  (LTO/STO) have been investigated<sup>12,13</sup>. Similarly as for  $\text{LaO}/\text{STO}$ , LTO/STO displays conducting behavior explained by electronic reconstruction, and superconductivity at low temperature<sup>13</sup>.  $\text{LaVO}_3$  (LVO) is another well known Mott insulator with antiferromagnetic order<sup>14</sup>. Thin films of LVO/STO were synthesized using the PLD technique by Hotta *et al.*<sup>15</sup>. Importantly, a pure LVO phase can be formed only under low partial pressure of oxygen (typ.  $< 10^{-5}$  Torr) and it is known that postannealing with oxygen quickly stabilizes the oxidized form of  $\text{LaVO}_4$ . Then it is likely that the problematic of oxygen vacancies has to be addressed in LVO/STO films. This heterostructure presents a conducting behavior and low temperature non linear Hall effect, which were explained by an intrinsic mechanism of electronic reconstruction at the interface<sup>16</sup>. The prime role of interface effects for explaining the LVO/STO metallic properties was also recently addressed<sup>17</sup>, and the role of oxygen vacancies was not considered since a STO substrate placed in the deposition chamber as a reference was not conducting after the ablation process. However, similar argument was shown to be non definitive at least in LAO/STO since

the presence of oxygen vacancies in STO is strongly enhanced by the presence of LAO deposited layers due to the contrast of activation energy for oxygen diffusion between the two materials<sup>7</sup>. The process of doping is then mainly driven by oxygen transfert between a growing film and its substrat<sup>18</sup>. Similar argument could *a priori* be applied in the LVO/STO case due to the difference in the diffusion for activation energy<sup>19</sup>. Other LVO/STO films were observed to be semiconducting-like<sup>20</sup>, what stress on the narrow window and strong sensitivity of transport properties in terms of oxygen partial pressure and the temperature used during the deposition. Here, we adress how the growth conditions affect the transport properties in a serie of high quality LVO/STO films, and the origin of the observed changes. Since the pressure can not be significantly change to stabilize  $\text{V}^{3+}$  in LVO, the most usefull parameter that can be tuned is the temperature growth. To do so, we have synthetised a series of high quality LVO thin films deposited on STO (001)-oriented substrates under different growth temperatures, and investigated both the structural and magnetotransport properties. By comparing the samples, we show that the transport properties are dominated by a semiconducting-metallic competition which is sensitive to the temperature growth. This can be explained using the contribution of the STO substrate doped by thermally activated oxygen vacancies, that appears to be a generic process in STO based heterostructure.

Epitaxial  $\text{LaVO}_3$  (LVO) thin films were prepared by the pulsed laser deposition technique on (001)-oriented  $\text{SrTiO}_3$  (STO) substrates (cubic with  $a=3.905$  Å). Briefly, a KrF laser ( $\lambda = 248\text{nm}$ ) with a repetition rate of 2 Hz was focused onto a  $\text{LaVO}_4$  polycrystalline target at a fluence of  $\simeq 2\text{J}/\text{cm}^2$ . The substrate is kept at a temperature ranging from  $600\text{-}750^\circ\text{C}$  under a dynamic vacuum around  $10^{-5}$  mbar. The target-substrate distance is fixed at 8.5 cm. The number of pulses was adjusted to obtain the desired thickness of 100 nm. conditions are similar as in<sup>21</sup> The X-ray diffraction measurements were performed with a  $\theta/2\theta$  diffractometer Seifert XRD 3000P ( $\lambda_{\text{Cu}}=1.5406$  Å) for room

temperature measurements and with a  $\theta/2\theta$  X'pert Pro MPD PANalytical ( $\lambda_{Co}=1.789$  Å) for measurements at different temperatures. The LVO structure is orthorhombic ( $Pnma$  (#62)) in its bulk form at room temperature and it undergoes a structural transition below 140K into a monoclinic ( $P2_1/c$  (#11)) symmetry<sup>22</sup>. Previously, we have shown that similar LVO thin film grown at 700°C presents a distorted orthorhombic structure due to the compressive stress induced by STO, with original  $VO_6$  rotations<sup>21</sup>.

Transport and galvanomagnetic properties were measured using a Quantum Design PPMS with the Van Der Pauw technique. Electrical contacts were realized using Al/Au wire-bonder. Sheet resistivity is defined as usual as  $R_s=\rho/t$ ,  $\rho$  being the bulk resistivity and  $t$  the thickness. The absorbance spectra were obtained using a Perkin Elmer spectrophotometer Lambda 1050. A 150 mm diameter Spectralon integrating sphere in total reflectance mode was used. Both the specular and diffuse reflectance components were collected on a R955 photomultiplier tube.

### A. Results.

Figure 1 depicts the  $\theta$ - $2\theta$  X-ray diffracted pattern of the LVO films grown at different temperatures and with different thicknesses. The sharpness of the peaks and the presence of Laue fringes confirm high structural quality, and a low interface roughness in agreement with previous reports<sup>23,24</sup>. As the growth temperature increases, the peak associated to LVO shifts towards higher  $2\theta$  angle, indicating a decreasing out of plane parameter. A similar c-axis expansion effect is known to be induced oxygen vacancies induced by low oxygen partial pressure during film deposition in copper oxides films<sup>25</sup>, and such effect has been recently discussed as relevant in  $PrVO_3$  films grown on STO<sup>26</sup>.

The resistance of the films was measured as a function of the temperature  $T$  (See Fig.2). LVO is a localized system with semiconducting conductivity<sup>42</sup> even in the presence of cationic and/or oxygen vacancies<sup>27,28</sup>, and stoichiometric STO are insulating, the low temperature data shows obvious metallic behavior with  $(dR/dT)>0$  up to a temperature  $T^*$ . For  $T>T^*$ ,  $dR/dT<0$  indicating semiconducting-like behavior.  $T^*$  varies for samples with different temperature growth with no obvious correlation. Room temperature values of sheet resistances  $R_s$  varies from  $R_s \sim 2.71$  to  $28.5 K\Omega/\square$  at room temperature to reach values as low as  $71 \Omega/\square$  for the most conducting sample. The order of magnitude are in the intermediate range of heterostructures (LTO/STO<sup>13</sup>, LAO/STO<sup>3</sup>) where low dimensional conduction and superconductivity has been discussed, and close to values reported in LVO/STO<sup>16,17</sup>.

An upturn of the resistance at low temperatures was reported by Hotta *et al* and was explained by an incipient localization<sup>16</sup>. We do not observe similar behavior

probably due to a smaller amount of defects in agreement with the lowest residual resistivity ( $\sim 70\Omega/\square$ ) that we measure.

To understand the origin of the change of conducting mechanism at  $T^*$ , we focus on the film grown at 700°C (Fig.3) where  $T^* \sim 225K$ . Since the film presents a distorted orthorhombic structure with significant tilts of  $VO_6$  octaedra at room temperature<sup>21</sup>, it is worth asking if the thermal variation of transport properties correlates with changes in lattice parameters and/or structural distortion<sup>29</sup>. In particular, it is not known if the orthorhombic to monoclinic observed at 140 K in bulk samples<sup>22</sup> is preserved in the thin film form of LVO. Note however that such transition favors orbital ordering and a more localized state<sup>30</sup>, hardly compatible with the low temperature metallicity observed here. The evolution of the out-of-plane lattice parameter of the film was recorded as function of temperature under cooling conditions (Fig. 3(b)). If small changes can be observed over a broad temperature range, there is no discontinuous changes that could indicate a transition and the temperature of c-axis minimum is shifted 60K from  $T^*$  (Fig. 3(b)). We conclude that the apparent semiconducting-metal is likely unrelated to the structural evolution of the LVO film.

To go further, we have investigated in details the galvanomagnetic properties of the same sample, and have measured the magnetoresistance MR and Hall effect at different fixed temperature.

As shown in Fig. 4, a positive MR is observed at low temperature which reaches  $MR(14T)=\frac{R(14T)-R(0T)}{R(0T)} \sim 0.01$  at 10K. It decreases continuously when increasing the temperature, as expected for metallic MR driven by mean free path effects. It increases notably in magnitude for  $T \lesssim 100K$ . We will return to this point later. Note that a drastic change of MR can be expected at a metal to insulator transition due to Fermi surface reconstruction. We observe here that the MR indeed changes sign at high temperature, but only very continuously and at a temperature larger than  $T^*$  (Inset of Fig. 4). This confirms that  $T^*$  corresponds to a smooth cross-over between two conducting regimes rather than a genuine transition.

We have measured the Hall resistance  $R_{xy}$  at various temperatures. It is found negative indicating n-type carriers with our experimental geometry. First analysis have been made using a single band model and fitting the data in the low field regime where  $R_{xy}$  is a linear function of the applied field. The mobility  $\mu$  and the sheet carrier density  $n_s$  have been then extracted as a function of the temperature and the results are reported in Fig. 5. We deduce electronic mobilities and carrier sheet density of respectively  $\mu \approx 1.3 \cdot 10^3 \text{ cm}^2/\text{V.s}$  and  $n_s \approx 2 \cdot 10^{13} / \text{cm}^2$  at low temperature. The obtained mobilities are consistent with the high values reported in other STO based heterostructures, including LVO/STO, deposited under low pressure. Such large values of mobilities are also characteristics of single phase STO doped by oxygen vacancies, as already discussed<sup>6,8</sup>.

When looking closely at the  $R_{xy}(B)$  curves, a non-linear field variation of the hall resistance can be evidenced. The non linearity is specially obvious for  $T < 100$  K. A non linear Hall resistance was observed by Hotta *et al.*<sup>16</sup> in conducting LVO/STO at low temperature and was proposed to arise from spin effects such as antiferromagnetic fluctuations at the interface<sup>16</sup> or strong spin orbit coupling<sup>31</sup>. In other heterostructures, similar non linear effect was also analyzed with a conventional galvanomagnetic coupling, but using a two bands rather than a single band model (<sup>32,33</sup> in LTO/STO,<sup>34</sup> in LAO/STO). Here, the field variation starts to be non linear at similar field and temperature for both the Hall and longitudinal resistance. This is in favor of an explanation in terms of galvanomagnetic coupling.

Within a two band model, two groups of charge carriers with mobilities  $\mu_1$  and  $\mu_2$  and densities  $n_1$  and  $n_2$  are considered. In this case, the Hall coefficient  $R_H = \frac{R_{xy}}{B}$  can be written as<sup>35</sup>:

$$R_H = 1/e \frac{n_1\mu_1^2 + n_2\mu_2^2 + (n_1 + n_2)\mu_1^2\mu_2^2 B^2}{(n_1\mu_1 + n_2\mu_2)^2 + (n_1 + n_2)^2\mu_1^2\mu_2^2 B^2} \quad (1)$$

To constraint the fit, we use the approach used in<sup>36,37</sup> by rewriting equation (1) as

$$R_H = \frac{R_0 + R_\infty \mu_*^2 B^2}{1 + \mu_*^2 B^2} \quad (2)$$

which has two fitting parameters  $\mu^*$  and  $R_\infty$ ,  $R_0$  being the zero field limit of  $R_H$  which is graphically determined. With the value of the zero field resistivity  $R_{xx} = (e.n_1.\mu_1 + e.n_2.\mu_2)^{-1}$ , the following equations gives four independant parameters  $\mu_1$ ,  $\mu_2$ ,  $n_1$  and  $n_2$

$$\begin{aligned} A &= (R_0/R_{xx} + \mu_*)/2 \\ \mu_1 &= A + (A^2 - \mu_* R_\infty/R_{xx})^{1/2} \\ \mu_2 &= A - (A^2 - \mu_* R_\infty/R_{xx})^{1/2} \\ C &= (\mu_1/\mu_2)(\mu_* - \mu_2)/(\mu_1 - \mu_*) \\ n_1 &= \frac{1}{eR_\infty(1+C)} \\ n_2 &= \frac{C}{eR_\infty(1+C)} \end{aligned} \quad (3)$$

Analysis of the data using this two-Bands model is very satisfactory, as demonstrated by the good fits reported in the fig 6.

The extracted parameters for all temperatures are shown in the fig 7. At low temperature, we find a carriers densities ratio  $n_1/n_2 \approx 0.14$  and mobilities ratio  $\mu_1/\mu_2 \approx 3.2$ . One open question is if the two bands scenario arises from spatially separated carriers with one of the carriers family located at the interface of the heterostructure<sup>33</sup>. Another possibility is that these different carriers are intrinsic to STO due to its complex electronic band structure with at least the presence of one heavy and one light

electron band<sup>38,39</sup>. The relevance of this two band scenario intrinsic to STO was recently confirmed by Laukhin *et al* based on measurements and analysis of the pressure dependence of electronic mobilities and carrier density<sup>40</sup>. From litterature, one expects at low temperature a ratio of effective mass  $m_1/m_2 \sim 10$ -20<sup>41</sup>. The mobilities are related to effective mass by  $(\mu_2/\mu_1) \sim (m_1/m_2)^q$  with  $q$  a constant dependant of the scattering mechanism<sup>35</sup>. For a dominant charged impurity scattering at low temperature,  $q=1/2$  and then  $(\mu_2/\mu_1) \sim 3.1$ -4.4 in very good agreement with our result. Then the contribution of STO alone is sufficient to account for non linear Hall effect in LVO/STO, and possibly in other heterostructures.

In the following, we will assume that the STO substrate is at least partially conducting. We propose a simple model to quantify this effect and to explain the macroscopic transport properties including the apparent metal to semiconducting transition. With our deposition condition, the low pressure ( $\sim 10^{-5}$  mbar) used during the LVO growth induces oxygen vacancies in the deposited layers. Their diffusion is thermally activated, and the high temperature ( $T_{Growth} > 600^\circ\text{C}$ ) used during the film deposition allows for their effective migration. As a key point, the oxygen vacancies are generated in the deposited layers and moves in STO due to its low activation energy for vacancies diffusion<sup>7,19</sup>. This process is more efficient as the growth temperature increases. If a high temperature growth favors oxygen vacancies in the substrate, the deposited film is correlatively more close to its stoichiometry. The c-axis parameter is known to expand with the oxygen vacancies (c-axis expansion effect)<sup>25,26</sup>. Then we expect a decrease of the c-axis value with the growth temperature, as we observe experimentally. Small departure from perfect La/Va ratio can be favored from oxygen deficiency in LVO<sup>42,43</sup>. However, such non stoichiometry has only a small effect on the transport properties of LVO which is a robust semiconductor with only small Band gap changes<sup>28</sup>. Contrarily, it is well known that even very small doping of STO by oxygen vacancies makes this latter conducting<sup>8,10</sup>. We have then to deal with two resistors in parallel: the LVO film expected to be semiconducting like, and the STO substrate partially conducting. One assumption is that the conducting thickness of the STO will be fixed by the diffusion lenght of oxygen vacancies at the macroscopic scale, and then could be a strong function of the temperature growth. Note that parallel resistors with opposite temperature variation mimic an equivalent resistor with non monotonic temperature variation which presents a resistance maximum at some intermediate temperature<sup>44</sup>, in qualitative agreement with our measurements (Fig.2). To be more quantitative,  $G_i$ ,  $\rho_i$  and  $t_i$  will stand for conductance, resistivity and thickness, and  $i=1,2$  are the LVO and STO, respectively. For a parallel resistor, the equivalent conductance  $G$  is:

$$G = \frac{1}{R} = G_1 + G_2 = \frac{1}{R_1} + \frac{1}{R_2} = \frac{t_1 L}{d\rho_1} + \frac{t_2 L}{d\rho_2} \quad (4)$$

While  $t_1 = 100\text{nm}$  is the physical thickness of LVO,  $t_2$  is an effective thickness corresponding to the conducting part of STO and related to the oxygen vacancies diffusion length  $\ell$ . Of course, using this crude modelling with two conducting blocks, we neglect interface effects that could additionally contribute to conducting processes. They can be *a posteriori* added if necessary. We neglect also finite size effects and boundary scattering that could occur in superlattices with thinner layers. For all samples, the low temperature resistance  $R(T)$  can be fitted by  $R_{res} + A.T^2$  ( $R_{res}$  is the residual resistance) over a large temperature range what is typical of a doped-STO contribution (Fig. 8). This indicates that the conducting paths are short-circuited by the substrate at low temperature ( $G_2 \ll G_1$ ) and  $R \sim R_2$  for  $T < \text{typ. } 100\text{K}$ . Assuming that  $R_2(T) = R_0 + A.T^2$  is fulfilled up to 300 K as in bulk STO,  $R_1(T)$  and  $\rho_1(T)$  are directly deduced using equation (4).

Conduction in bulk LVO is semiconducting-like with a resistivity described by a thermally activated law,  $\rho(T) \propto \exp(E_a/KT)$  ( $E_a$  the activation energy,  $K$  the Boltzmann constant). As shown in fig.8,  $R_1(T)$  follows indeed such an activated behavior, and we found similar behavior for all the growth temperature (Fig.9). The extracted activation energies  $E_a$  are found close to 0.2 eV, a very reasonable value for conducting processes in rare earth vanadates such as LVO<sup>42</sup>.  $\rho_1$  at room temperature are found to be in good agreement as the resistivity of bulk LVO<sup>42</sup>, and it increases when  $T$  decreases (Fig.9). Since the highest growth temperature favors the diffusion of oxygen vacancies in STO, their amount in LVO is expected to be larger at 600°C than at 750°C. In one hand, the presence of oxygen vacancies or charge defects can reduce the resistance by doping and/or by creating mixed valencies in STO. In LVO, we observe at contrary an increase of resistance with oxygen non-stoichiometry. However, there is no contradiction with the litterature since the introduction of mixed valency in LVO by non stoichiometry processes favors carriers localization by the creation of defect states<sup>28</sup>. Finally, we conclude that  $R_1$  is the resistance the LVO film.

Let us now return to the behavior of STO. The oxygen vacancies diffusion mechanism is a thermally activated

process, with a diffusion constant given by an Arrhenius dependence  $D(T) = D_0 \exp(-U/KT)$  where  $D_0$  is the diffusion constant,  $U$  the activation energy. Then during a growth time  $\tau_d$  and at a temperature  $T_{growth}$ , the diffusion length is  $\ell(T_{growth}) = \sqrt{D(T_{growth}) \times \tau_d}$ . At a first approximation, the effective thickness of conducting STO can be written as  $t_2 \sim \ell$ . Dealing with the room temperature values of conductivity, we neglect here the possible spreading of carriers due to the unusual large dielectric constant of STO at low temperature<sup>8</sup> which was challenged in<sup>10</sup>. At room temperature and below, we assume also that the thermal energy (typ. 0.026 eV at 300K) is low enough to neglect any supplementary vacancies diffusion. Finally, one finds that the STO conductance  $G_2$  is

$$G_2 = 1/R_2 \sim \sqrt{D_0 \exp(U/KT_{growth}) \tau_d / \rho_2} \quad (5)$$

Here the important parameter is  $U$ , the activation energy for diffusion of oxygen vacancies in STO, which is experimentally given by the slope of  $\ln(G_2)$  as function of  $1/T_{growth}$  (Fig. 10). The fit gives  $U \sim 0.9$  eV which is very reasonable comparing with litterature ( $U \sim 0.7 - 1.4$  eV)<sup>45,46</sup>.

In conclusion, we have studied galvanomagnetic properties on a serie of  $\text{LaVO}_3$  thin films grown on  $\text{SrTiO}_3$ . We observe that, as it was reported for similar and other heterostructures based on STO substrate, pronounced metallic character with very large electronic mobilities is observed. Additionnally, a non monotonic temperature variation of resistance is observed with a strong influence of temperature growth. We present evidence that that the growth temperature modifies the substrate oxydation and its conductivity. As a consequence, the measured film behaves as a parallel-like resistor with semiconducting LVO and metallic STO resistances. Even though electronic reconstruction effects might be present in the system, the macroscopic electronic transport properties, including non linear Hall effect, are mainly driven by the competition between these two bulk components, with a strongly dominating role of STO at low temperature.

<sup>1</sup> A. Ohtomo and H. Y. Hwang, Nature 427, 423 (2004)

<sup>2</sup> N. Reyren, S. Thiel, A.D. Caviglia, L.F. Kourkoutis, G. Hammerl, C. Richter, C.W. Schneider, T. Kopp, A.S. Rüetschi, D. Jaccard, M. Gabay, D.A. Muller, J.M. Triscone, and J. Mannhart, Science 317, 1196 (2007)

<sup>3</sup> A.D. Caviglia, S. Gariglio, N. Reyren, D. Jaccard, T. Schneider, M. Gabay, S. Thiel, G. Hammerl, J. Mannhart, and J.-M. Triscone, Nature (London) 456, 624 (2008)

<sup>4</sup> N. Nakagawa, H.Y. Hwang, and D.A. Muller, Nat. Mater. 5, 204 (2006)

<sup>5</sup> S. Thiel, G. Hammerl, A. Schmehl, C.W. Schneider, and J. Mannhart, Science 313, 1942 (2006).

<sup>6</sup> G. Herranz, M. Basletic, M. Bibes, C. Carretero, E. Tafr, E. Jacquet, K. Bouzehouane, C. Deranlot, A. Hamzic, J.-M. Broto, A. Barthélémy, and A. Fert, Phys. Rev. Lett. 98, 216803 (2007)

<sup>7</sup> A. Kalabukhov, R. Gunnarsson, J. Borjesson, E. Olsson, T. Claeson, and D. Winkler, Phys. Rev. B 75, 121404(R) (2007)

<sup>8</sup> W. Siemons, G. Koster, H. Yamamoto, W. A. Harrison, G. Lucovsky, Th.H. Geballe, D.H.A. Blank, and M.R. Beasley, Phys. Rev. Lett. 98, 196802 (2007)

<sup>9</sup> M. Basletic, J.-L. Maurice, C. Carretero, G. Herranz, O. Copie, M. Bibes, E. Jacquet, K. Bouzehouane, S. Fusil and

- A. Barthelemy, *Nature Mater.* 7, 621 (2008)
- <sup>10</sup> O. Copie, V. Garcia, C. Bodefeld, C. Carretero, M. Bibes, G. Herranz, E. Jacquet, J.-L. Maurice, B. Vinter, S. Fusil, K. Bouzehouane, H. Jaffres, and A. Barthelemy, *Phys. Rev. Lett.* 102, 216804 (2009)
- <sup>11</sup> S. Okamoto and A.J. Millis, *Nature* 428, 630 (2004)
- <sup>12</sup> A. Ohtomo, D. A. Muller, J. L. Grazul, and H. Y. Hwang, *Nature* 419, 378 (2002)
- <sup>13</sup> J. Biscaras, N. Bergeal, A. Kushwaha, T. Wolf, A. Rastogi, R.C. Budhani, J. Lesueur, *Nature Communications* 1, 1 (2010).
- <sup>14</sup> A. V. Mahajan, D. C. Johnston, D. R. Torgeson, and F. Borsa, *Phys. Rev. B* 46, 10966 (1992)
- <sup>15</sup> Y. Hotta, Y. Mukunoki, T. Susaki, H. Y. Hwang, L. Fitting and D. A. Muller, *Appl. Phys. Lett.* 89, 031918 (2006)
- <sup>16</sup> Y. Hotta, T. Susaki, and H.Y. Hwang, *Phys. Rev. Lett.* 99, 236805 (2007)
- <sup>17</sup> C. He, T. D. Sanders, M. T. Gray, F. J. Wong, V. V. Mehta, and Y. Suzuki, *Physical Review B* 86, 081401 (2012)
- <sup>18</sup> W. Schneider, M. Esposito, I. Marozau, K. Conder, M. Doebeli, Yi Hu, M. Mallepell, A. Wokaun and T. Lippert, *Appl. Phys. Lett.* 97, 192107 (2010)
- <sup>19</sup> M. Cherry, M.S. Islam and C.R.A. Catlow, *J. Solid State Chem.* 188, 125 (1995)
- <sup>20</sup> W.C Sheets, B. Mercey, W. Prellier, *Appl. Phys. Lett.* 91, 192102 (2007)
- <sup>21</sup> H. Rotella, U. Luders, P.-E. Janolin, V. H. Dao, D. Chateigner, R. Feyerherm, E. Dudzik, and W. Prellier *Physical Review B* 85, 184101 (2012)
- <sup>22</sup> P. Bordet, C. Chaillout, M. Marezio, Q. Huang, A. Santoro, S-W. Cheong, H. Takagi, C.S. Oglesby, B. Batlogg, *J. Sol. State Chem.* 106, 253 (1993)
- <sup>23</sup> P. Boullay, A. David, W. C. Sheets, U. Luders, W. Prellier, H. Tan, J. Verbeeck, G. Van Tendeloo, C. Gatel, G. Vincze, and Z. Radi, *Phys. Rev. B* 83, 125403 (2011)
- <sup>24</sup> Haiyan Tan, Ricardo Egoavil, Armand Beche, Gerardo T. Martinez, Sandra Van Aert, Jo Verbeeck, Gustaaf Van Tendeloo, Helene Rotella, Philippe Boullay, Alain Pautrat, and Wilfrid Prellier, *Phys. Rev. B* 88, 155123 (2013)
- <sup>25</sup> J.C. Cheang Wong, C. Ortega, J. Siejka, I. Trimaille, A. Sacuto, L.M. Mercandalli, F. Mayca, *Journal of Alloys and Compounds* 195 May, 675 (1993)
- <sup>26</sup> O. Copie, H. Rotella, P. Boullay, M. Morales, A. Pautrat, P-E Janolin, I. C. Infante, D. Pravathana, U. Luders and W. Prellier, *J. Phys.: Condens. Matter* 25, 492201 (2013)
- <sup>27</sup> H. Hur, S. H. Kim, K. S. Yu, Y. K. Park, J. C. Park, and S. J. Kim, *Solid ñ State Commun.* 92, 541 (1994)
- <sup>28</sup> S. Jamali Gharetape, M. P. Singh, F. S. Razavi, D. A. Crandles, L. Y. Zhao and K. T. Leung, *Appl. Phys. Lett.* 98, 052509 (2011)
- <sup>29</sup> A. David, R. Fresard, Ph. Boullay, W. Prellier, U. Luders and P.-E. Janolin, *Appl. Phys. Lett.* 98, 212106 (2011)
- <sup>30</sup> J.S. Zhou, Y. Ren, J.Q. Yan, J.F. Mitchell, and J.B. Goodenough, *Phys. Rev. Lett.* 100, 046401 (2008)
- <sup>31</sup> H. Weng and K. Terakura, *Phys. Rev. B.* 82, 115105 (2010)
- <sup>32</sup> J. S. Kim, S. S. A. Seo, M. F. Chisholm, R. K. Kremer, H.-U. Habermeyer, B. Keimer, and H. N. Lee, *Phys. Rev. B* 82, 201407 (2010)
- <sup>33</sup> J. Biscaras, N. Bergeal, S. Hurand, C. Grossetete, A. Rastogi, R. C. Budhani, D. LeBoeuf, C. Proust, and J. Lesueur, *Phys. Rev. Lett.* 108, 247004 (2012).
- <sup>34</sup> C. Bell, S. Harashima, Y. Kozuka, M. Kim, B. G. Kim, Y. Hikita, and H. Y. Hwang, *Phys. Rev. Lett.* 103, 226802 (2009)
- <sup>35</sup> J. M. Ziman, *Principles of the Theory of Solids*, Cambridge University Press, 1964.
- <sup>36</sup> E.K. Arushanov and G.P. Chuiko, *Phys. Status Solidi (a)* 17, K135 (1973)
- <sup>37</sup> R. Laiho, A.V. Lashkul, K.G. Lisunov, E. Lahderanta, M.O. Safonchik and M.A. Shakhov, *Semicond. Sci. Technol.* 19, 602 (2004)
- <sup>38</sup> L.F. Mattheiss, *Phys. Rev. B* 6, 4718 (1972)
- <sup>39</sup> M. Ahrens, R. Merkle, B. Rahmati and J. Maier, *Physica B* 393, 239 (2007)
- <sup>40</sup> V. Laukhin, O. Copie, M. J. Rozenberg, R. Weht, K. Bouzehouane, N. Reyren, E. Jacquet, M. Bibes, A. Barthél my, and G. Herranz, *Phys. Rev. Lett.* 109, 226601 (2012)
- <sup>41</sup> A. F. Santander-Syro, O. Copie, T. Kondo, F. Fortuna, S. Pailhes, R. Weht, X. G. Qiu, F. Bertran, A. Nicolaou, A. Taleb-Ibrahimi, P. Le Fevre, G. Herranz, M. Bibes, Y. Apertet, P. Lecoeur, M. J. Rozenberg, A. Barthelemy, *Nature* 469, 189 (2011)
- <sup>42</sup> D. B. Rogers, A. Ferretti, D. H. Ridgley, R. J. Arnott, and J.B. Goodenough, *J. Appl. Phys.* 37, 1431 (1966)
- <sup>43</sup> H. Seim and H. Fjellvag, *Acta Chem. Scand.* 52, 1096 (1998)
- <sup>44</sup> C. Grygiel, A. Pautrat, W. Prellier, B. Mercey, W. C. Sheets, and L. Mechin, *J. Phys.: Condens. Matter* 20, 472205 (2008).
- <sup>45</sup> P.Pasierb, S. Komornicki, and M. Rekas, *J. Phys. Chem. Sol.* 60, 1835 (1999)
- <sup>46</sup> R. De Souza, V. Metlenko, D. Park, and T. Weirich, *Phys. Rev. B* 85, 174109 (2012)

FIG. 1:  $\theta$ - $2\theta$  X-ray diffracted pattern of 100 nm thick films grown at 600, 650, 700 and 750°C, respectively. The star indicates the  $K_{\alpha 2}$  contribution of the diffractometer on the (002)SrTiO<sub>3</sub> reflection.

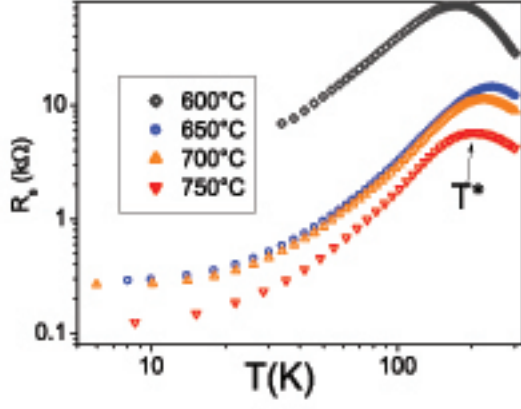


FIG. 2: Sheet resistance  $R_s$  of the samples grown at different temperature in a log-log scale. Note the maximum of resistance at  $T^*$ .

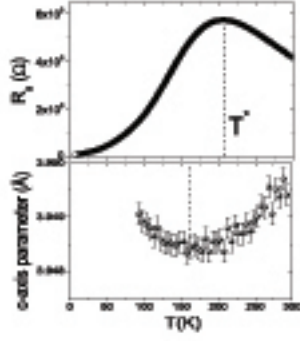


FIG. 3: (a) Variation of the sheet resistance of LVO/STO grown at  $700^\circ$ . Note the maximum at a temperature  $T^*$  signing a semiconducting-like to metallic change of conductivity. (b) out-of-plane lattice parameter as a function of the temperature. Note the large difference between  $T^*$  and the temperature where the c-axis parameter is minimum .

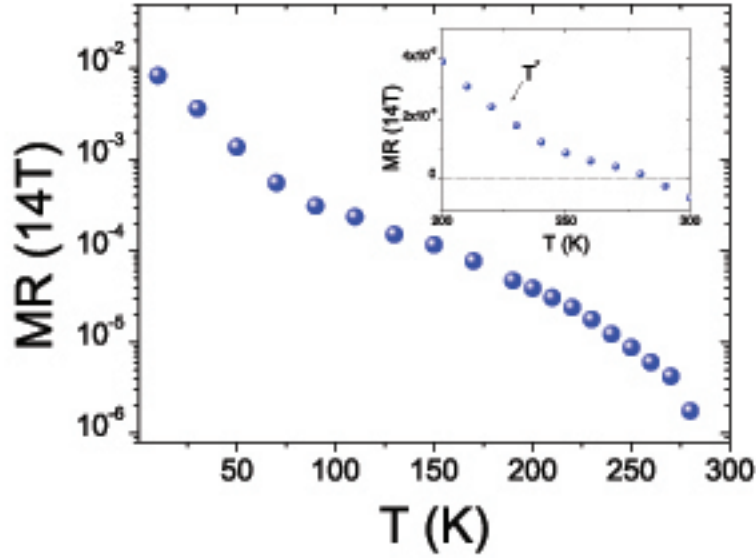


FIG. 4: Magnetoresistance at 14T vs. temperature in a log-linear scale. (the insert shows the cross-over between positive and negative MR a  $T > T^*$ ).

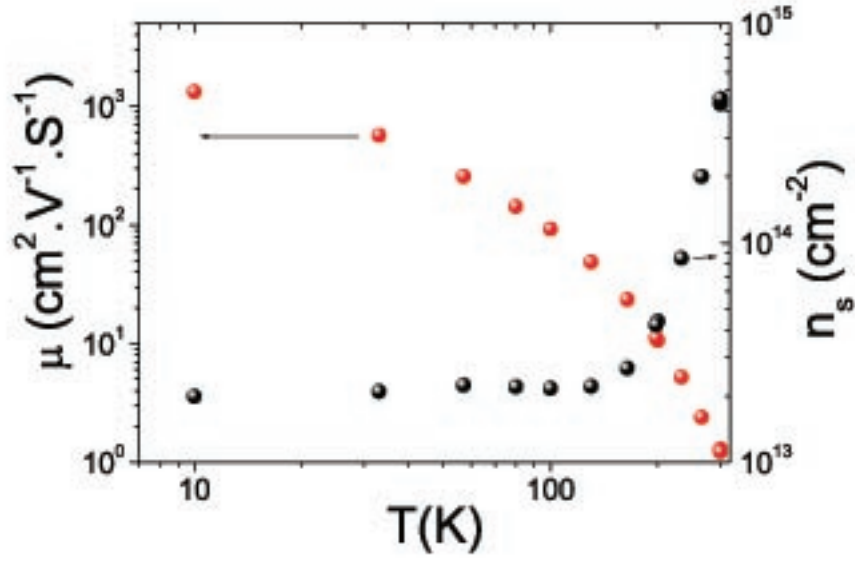


FIG. 5: Mobility and sheet carrier density deduced from the Hall measurements using a single carrier model.

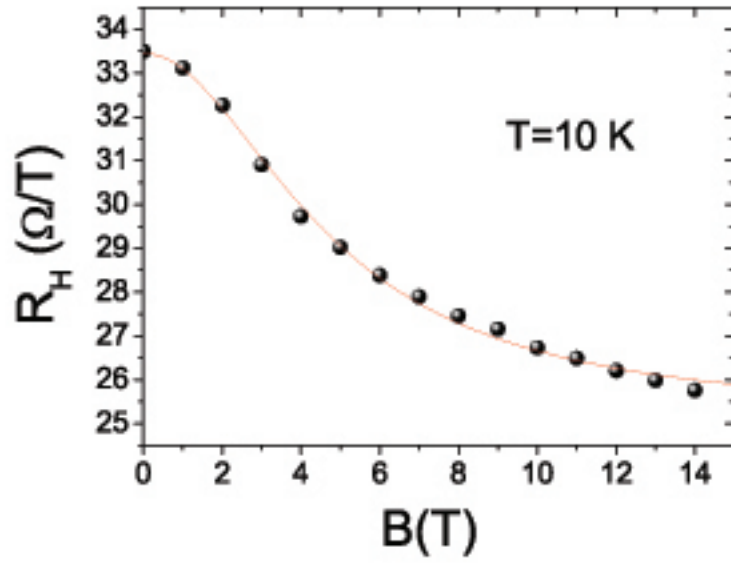


FIG. 6: Hall resistance  $R_H=R_{xy}/B$  versus the magnetic field  $B$  at  $T=10 \text{ K}$ . The solid line is a fit performed with the two bands Hall effect (equation (2)).



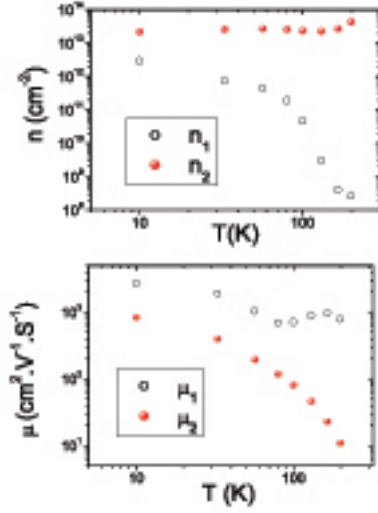


FIG. 7: Sheet carrier densities (top) and mobilities (bottom) of light and heavy carriers calculated from the two bands analysis.

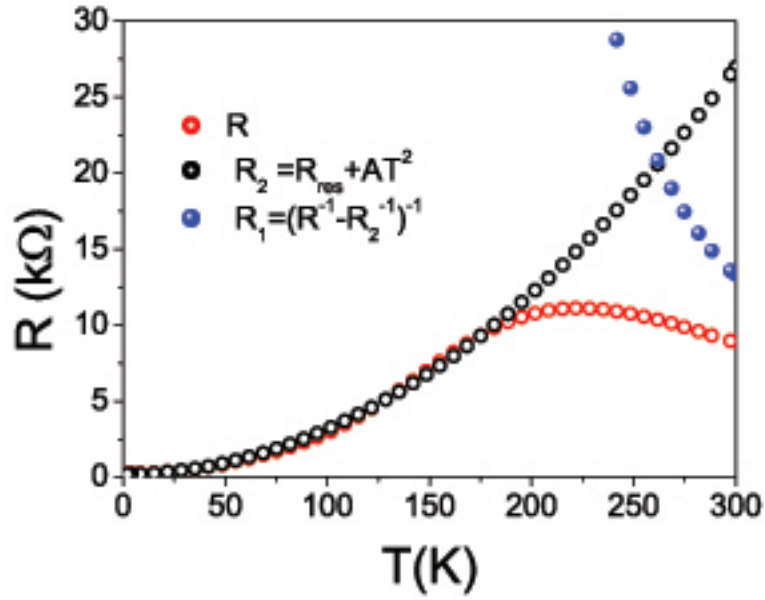


FIG. 8: Experimental  $R$  for the sample grown at 700 deg,  $R_1 = R_{res} + AT^2$  low temperature variation and the deduced  $R_1$  resistance using a parallel resistor modelling.

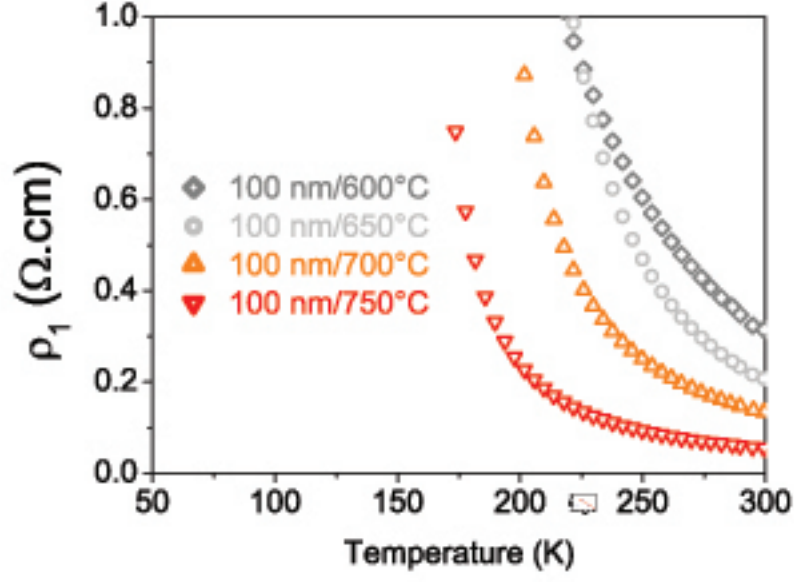


FIG. 9:  $\rho_1(T)$  deduced from the parallel resistor analysis and associated to the LVO component, for different temperature growth.

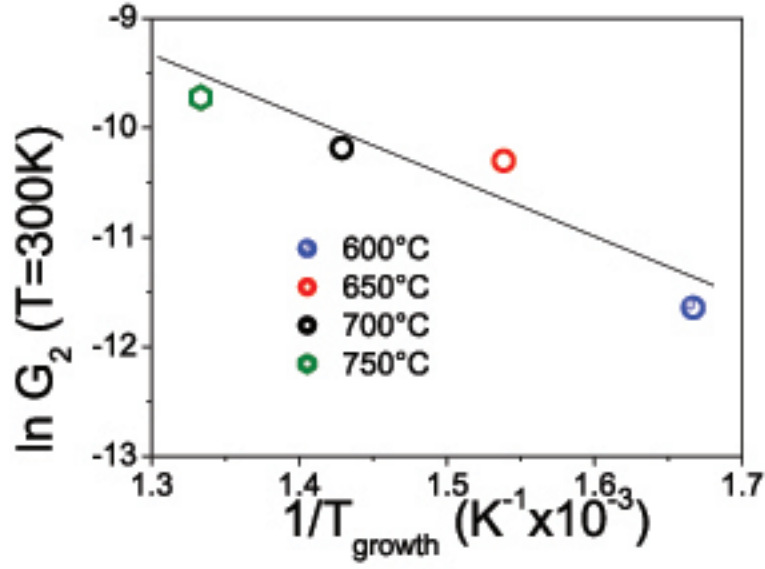


FIG. 10:  $\ln G_2$  as function of  $1/T_{growth}$  for all samples. The line corresponds to an activation energy of  $U/2 \sim 0.45$  eV.